

A comparative study of the mechanical properties of a dinosaur and crocodile fossil teeth

Lakshminath Kundanati^a, Mirco D'Incau^b, Massimo Bernardi^c, Paolo Scardi^b,
Nicola M. Pugno^{a,d,e,*}

^a Laboratory of Bio-inspired and Graphene Nanomechanics, Department of Civil, Environmental and Mechanical Engineering, University of Trento, 38123, Italy

^b Department of Civil, Environmental and Mechanical Engineering, University of Trento, Via Mesiano 77, 38123, Trento, Italy

^c MUSE – Museo delle Scienze di Trento, Corso del Lavoro e della Scienza 3, 38122, Trento, Italy

^d School of Engineering and Materials Science, Queen Mary University of London, Mile End Road, London, E1 4NS, United Kingdom

^e Ket-Lab, Edoardo Amaldi Foundation, Via del Politecnico snc, 00133, Roma, Italy

ARTICLE INFO

Keywords:

Suchomimus tenerensis

Sarcosuchus imperator

Microindentation

Nanoindentation

Scratch test

ABSTRACT

Vertebrate teeth are complex structures adapted in terms of shape and structure to serve a variety of functions like biting and grinding. Thus, examining the morphology, composition and mechanical properties of the teeth can aid in providing insights into the feeding behaviour of extinct species. We here provide the first mechanical characterisation of teeth in a spinosaurid dinosaur, *Suchomimus tenerensis*, and a pholidosaurid crocodylomorph, *Sarcosuchus imperator*. Our results show that both species have similar macrostructure of enamel, dental and interfacial layers, and similar composition, the main constituent being fluorapatite. Microindentation tests show that *Suchomimus* teeth have lower elastic modulus and hardness, as compared to *Sarcosuchus*. On the contrary, *Sarcosuchus* teeth have lower toughness. Nanoindentation showed the existence of mechanical gradients from dentin to enamel in *Suchomimus* and, less prominently, in *Sarcosuchus*. This was also supported by wear tests showing that in *Suchomimus* the dentin region is more wear-prone than the enamel region. With still scarce information available on the dietary regimes in extinct species, the analysis of micro and nano-mechanical properties of fossils teeth might be a help in targeting specific biological questions. However, much is still unknown concerning the changes underwent by organic material during diagenesis making at present impossible to definitely conclude if the differences in the mechanical properties of *Suchomimus* and *Sarcosuchus* here retrieved imply that the two species adopted different strategies when dealing with food processing or are the result of disparate taphonomic histories.

1. Introduction

Vertebrate teeth are adapted in terms of shape, size, position and mechanical properties to perform a variety of functions such as piercing and grinding, and the observed differences in various teeth are often species-specific. Palaeontologists routinely use tooth morphology to study extinct species because of the high probability of preservation with respect to other skeletal parts (Teaford et al., 2006). The fossil record is relatively rich in vertebrate teeth, which are used for bio-chronology, environmental and ecological characterization (via isotopic analysis of the enamel) and evolutionary studies. Teeth are known to possess excellent mechanical properties (Meyers et al., 2008), and several studies have highlighted the unique features of these complex

structural materials (He and Swain, 2009; Marshall et al., 2001; Poole, 1957). They are formed of two main bulk layers: enamel, the external hard layer, and dentin, the internal layer which is relatively softer. The Dentin Enamel Junction (DEJ) that forms the intermediate bonding layer between enamel and dentin, plays a key role in the overall function of the tooth (Shimizu and Macho, 2007). Thus, a detailed characterization of teeth can be done by determining and comparing the composition and properties of enamel, dentin, and DEJ.

Going beyond the classical external morphological comparison, a number of studies (Hwang, 2005, 2010, 2011) recently investigated the internal dental structure of several extinct vertebrate species, and dinosaurs in particular, by looking at the ultrastructure and performing mechanical simulations. Together with biomechanical studies of

* Corresponding author. Laboratory of Bio-inspired and Graphene Nanomechanics, Department of Civil, Environmental and Mechanical Engineering, University of Trento, 38123, Italy.

E-mail address: nicola.pugno@unitn.it (N.M. Pugno).

<https://doi.org/10.1016/j.jmbbm.2019.05.025>

Received 26 October 2018; Received in revised form 15 May 2019; Accepted 16 May 2019

Available online 18 May 2019

1751-6161/ © 2019 Elsevier Ltd. All rights reserved.

mandibles, snouts or entire skulls (Rayfield et al., 2001; Rayfield, 2007; Fortuny et al., 2012; Serrano-Fochs et al., 2015), these works helped in building an entirely new depiction of biomechanical capabilities and habits, in particularly feeding behaviour.

Some of these studies have tried to answer a long-standing question of whether the overall morphological similarity between the snout of a Cretaceous group of theropod dinosaurs, the spinosaurids, and that of long-snouted crocodiles is in some way mirrored by similar biomechanical behaviour (Cuff and Rayfield, 2013; Rayfield et al., 2007; Therrien, 2005; Rayfield, 2011). The Spinosauridae (Serenó et al., 1998) show a characteristic low, elongated skull and mandible that is reminiscent of a long snout exhibited by some extinct and extant crocodilians, such as the Indian gharial (*Gavialis gangeticus*) or the Orinoco crocodile (*Crocodylus intermedius*). This similarity is often referred to as “crocodile-mimic” (e.g. Rayfield et al., 2007; Holtz, 1998) and has been repeatedly used in the past to infer a similar morpho-functional relationship implying possible analogous piscivorous feeding behaviour (Rayfield et al., 2007; Sereno et al., 1998). Present-day knowledge, supported by classical direct evidence on the fossil specimens (Holtz, 1998; Martill et al., 1996; Charig and Milner, 1997; Buffetaut et al., 2004), virtual biomechanical approaches like finite element (FE) models (Rayfield, 2007), and beam theory (Cuff and Rayfield, 2013; Therrien, 2005), posits that spinosaurids were not obligate piscivorous and could have fed also on small terrestrial prey, with species-specific adaptations. They probably used the anterior portion of their jaws to manipulate prey (Sues et al., 1999) though, some species could resist well in bending and torsion (e.g. *Suchomimus tenerensis*, Therrien, 2005), while some other had lower performance (e.g. *Baryonyx walkeri*, Rayfield, 2007), and some others derived their biting force from their huge body size rather than specific skull adaptations e.g., *Spinosaurus aegypticus* (Cuff and Rayfield, 2013).

The goal of our study is to provide a mechanical characterisation of teeth in spinosaurid dinosaurs and the long-snouted crocodiles. To address these questions, we determined for the first time, elastic modulus, hardness, scratch resistance and fracture toughness in the dentin and enamel of maxillary teeth in a spinosaurid, *Suchomimus tenerensis* (Serenó et al., 1998), and a crocodile, *Sarcosuchus imperator* (Serenó et al., 2001). These two species were selected because they co-existed, having lived in the very same fluvial environment of the North African Aptian (Lower Cretaceous, ca. 120 Ma) now documented by the Gadoufaoua Elrhaz Formation of Niger (Taquet, 1976), and because whole-body biometric and morphological comparison allows us to hypothesise similar dietary regimes and occupation of the same ecological niche, suggesting potential competition. Furthermore, unlike other theropods, spinosaurid teeth have a subcircular-elliptical cross-section (Hendrickx et al., 2015) similar to those of *Sarcosuchus* (Kellner and Mader, 1997) therefore allowing meaningful comparison of structures with similar external morphology.

2. Materials and methods

2.1. Specimens

In this work we compare the teeth of two distinct species collected in the same stratigraphic horizon of the Elrhaz Formation of Niger (Taquet, 1976) during field work of the Museo di Storia Naturale di Milano, Italy (MSNM here hence) in 1980. We have used one sample tooth from each of the two species, because of the unavailability of more than one specimen for destructive analysis. MSNM V6313 is a spinosaurid dinosaur maxillary tooth attributed to the species *Suchomimus tenerensis* (Serenó et al., 1998), which belong to the family Baryonychinae. MSNM V6288 is a crocodile maxillary tooth assigned to the species *Sarcosuchus imperator* (Serenó et al., 2001). In the absence of a detailed revision, following previous works (Hendrickx et al., 2016) we keep the name *S. tenerensis* although it is probably a junior synonym of *Cristatusaurus lapparenti* (Taquet and Russell, 1998).

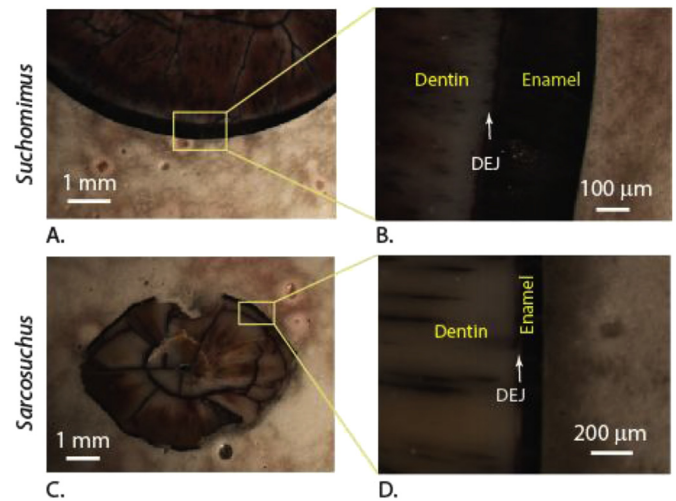


Fig. 1. Optical micrographs of the cross-sections showing different constitutive layers: A-B) *Suchomimus* C-D) *Sarcosuchus*.

2.2. Sample preparation

All tooth samples were embedded in a resin (Technovit® 4002 IQ) and polished using a series of 400, 800, 1200, 2000 and 4000 grade sand papers. We have polished the samples from labial side to the lingual side, by changing the direction by 90° in consecutive sessions. Finally, the sample was polished using a diamond paste of particle sizes in the range of 6 μm and 1 μm, to obtain a scratch free surface. Fig. 1 shows the polished tooth sections.

2.2.1. Microscopy

Images of tooth cross-sections were captured using an optical microscope (Lynx LM-1322, OLYMPUS) attached with a CCD camera (Nikon). The embedded cross-sections samples were carefully mounted on double-sided carbon tape, stuck on an aluminum stub followed by sputter coating (Manual Sputter Coater, AGAR SCIENTIFIC) with gold. Imaging was carried out using a SEM (EVO 40 XVP, ZEISS, Germany) with accelerating voltages between 5 and 10 kV, and in Secondary Electron Imaging mode. ImageJ software was used for all dimensional quantification reported in this study (Abramoff and Magalhães, 2004).

2.2.2. X-ray microanalysis and X-ray diffraction

X-ray microanalysis and X-ray diffraction were used to test the comparability of the samples (i.e. the composition as a result of the taphonomic processes underwent since their burial in the sediment). The embedded and polished samples of the teeth were sputter coated with gold layer to perform microanalysis using the EDAX detector (Aztec, Oxford Instruments, United Kingdom) attached to the SEM (EVO 40 XVP, ZEISS, Germany). A high voltage of 20 kV and working distance of 10 mm was used to ensure optimum amount of counts during the analysis. For quantification of elements, we have used spot analysis. For microstructural examination the sectioned samples were polished and their surfaces were etched with 5% v/v HCl for 3 min. After etching the samples were thoroughly cleaned with de-ionised water and followed by ultrasonication for 2 min.

The corresponding dentin and enamel regions were carefully scrapped to remove some fragments. These fragments were then ground to fine powder using a ceramic mortar and pestle. The fine powder was spread on a flat silicon wafer and then exposed to the X-ray beam of MoK_α radiation in the diffractometer (ARL™ XTRA Powder Diffractometer, Thermo Fisher SCIENTIFIC) with a voltage of 45 kV and a current of 40 mA, and a Si-Li solid state detector to record the diffracted intensity. The specimens were then scanned between the 2θ range of 9–31° with a sampling step of 0.05°, a counting time of 15 s,

and using a slit of 0.5 deg. In order to identify peaks, we used the peaks given in database ICDD PDF (card #15–0876 for fluorapatite ($\text{Ca}_5(\text{PO}_4)_3\text{F}$, hexagonal)).

2.2.3. Microindentation and nanoindentation

We used both microindentation and nanoindentation testing because of their different capabilities. Microindentation was used to estimate the mechanical properties, primarily to measure the fracture toughness because nanoindentation could not provide sufficiently long enough crack that can be measured easily. Nanoindentation was used to capture regional differences in terms of mechanical property maps, mainly elastic modulus and hardness. Microindentation experiments were performed using a standard CSM micro indenter with a load application 200 mN and at a loading rate of 200 mN/min. A standard Vickers indenter was used for measuring the properties. The maximum applied load for indentation was chosen either by minimum detectable indentation impression visible through the microscope or a load that could make an indentation without resulting in catastrophic cracking of the sample surface. Poisson ratio of 0.31 was used for estimating the modulus (Rubin et al., 1985). Scratch experiments were performed using a maximum load until a visible wear track was observed on the specimen surface. Using these tests, the wear behaviour of the samples was assessed using depth of scratch. To determine the fracture toughness of the teeth, the same samples were indented using much higher load of 2 N at a rate of 2 N/min to create fracture around the indentation region. In nanoindentation experiments (using iNano, Nanomechanics, Inc., USA), Berkovich indenter was used to perform indentations up to a maximum load of 30 mN which allowed us to find visible indentation, and at the rate of 1.8 N/min. NanoBlitz3D software was used to map the cross-sectional surface of the tooth samples.

We estimated the fracture toughness of materials by using the measured mechanical properties and the crack length dimensions using the images post indentation. Fracture toughness K_{IC} was estimated using classical Lawn Evans Marshall model (Lawn and Wilshaw, 1975; Evans et al., 1976):

$$K_{IC} = \alpha \left(\frac{E}{H} \right)^{0.5} \left(\frac{P_{max}}{c^{3/2}} \right) \quad (1)$$

where here $\alpha = 0.016$ (for quasi-brittle materials), E is the Young modulus, H is the hardness, P_{max} is the maximum load and c is the crack length.

The largest crack was used to determine the crack length c (taken from the center of the indentation impression to the crack tip, considering the longest crack for a specific indentation) for estimation of toughness.

3. Results

3.1. X-ray microanalysis and X-ray diffraction

X-ray microanalysis was carried out both in the dentin and enamel regions to determine the elemental composition qualitatively. Spectra from these results showed that both regions contained primarily calcium (Ca), potassium (P), oxygen (O), carbon (C), silicon (Si) and traces of fluorine (F), sodium (Na) (Fig. 2A and B). The gold peak comes from the sputter coating used to make the surface conducting. Qualitatively we found no significant differences in the elements present in the teeth of the two species (Table 1).

Notably the amount of the silicon was significantly less than 1 wt% in both species. The only minor difference observed between the two teeth was a slightly higher wt% of fluorine and sodium contents in the *Sarcosuchus* tooth (Table 1). When comparing the internal variations, we observed that the fluorine concentration was higher in dentin region of the teeth (Table 2). The Ca/P ratio was ~ 2 in dentin and enamel regions of both the species (Table 2).

X-ray powder diffraction technique was used to examine the crystalline materials present in the tooth regions. The majority of the significant intensity x-ray peaks from these experiments primarily matched with fluorapatite (Fig. 3A and B) and all are comparable (nearly identical) between samples.

3.2. Microstructure

Scanning electron microscopy highlighted microstructural similarities and differences in the teeth. Dentin tubules were observed in both species both in axial and sagittal planes (Figs. 4A and 5A).

The dentin crystallites in both teeth are similar, as seen in the micrographs taken both in axial and sagittal planes (Fig. 4B and C and 5B–C). In both species, a clear demarcation was observed at the DEJ (Figs. 4D and 5D). In *Suchomimus*, DEJ appeared to have a wavy nature, probably to increase interface strength and toughness, unlike in *Sarcosuchus* (Fig. 4D). The enamel region in the *Suchomimus* shows that elongated prismless enamel crystallites were arranged in a curved path that is diverging (Fig. 4D and E). In *Sarcosuchus*, single prismless enamel crystallites are similar to those of *Suchomimus* but the wavy pattern was not observed (Fig. 5E). In both species prismless enamel crystallites are densely packed. High magnification electron micrographs show that enamel crystallites spanned length scales in the orders tens of nanometres to that of a few hundred nanometres (Fig. 4F and 5F).

3.3. Microindentation

Microindentation experiments were used to estimate Young modulus and hardness at microscale. The depth of penetration in all the experiments was observed to be in the range $\sim 1\text{--}2\text{ }\mu\text{m}$. Results show the difference between mechanical properties of the outer enamel layer and the inner dentin layer. The elastic modulus and hardness values were significantly higher in the enamel region as compared to the dentin region in *Suchomimus tenerensis*, while the difference was less significant in *Sarcosuchus imperator*. *Suchomimus* had lower values of elastic modulus (Dentin: 57 ± 13 , Enamel: 81 ± 12 GPa), and hardness (Dentin: 2.6 ± 0.8 , Enamel: 4.5 ± 2.7 GPa) in both regions. *Sarcosuchus* displayed higher values of elastic modulus (Dentin: 91 ± 9 , Enamel: 103 ± 11 GPa) and hardness (Dentin: 6.1 ± 0.4 , Enamel: 6.7 ± 1.2 GPa).

3.4. Nanoindentation

Nanoindentation experiments were used to map the properties in more detail with at least 200 indentations in each location. Indentation locations were selected to map the properties of dentin, transition region, and enamel layer. The property maps of *Suchomimus* show a clear gradation of elastic modulus and hardness from dentin layer to enamel layer, with a clear demarcation at the interface (Fig. 6A and C). The average elastic modulus and hardness in the dentin region were ~ 45 GPa and ~ 2.5 GPa, as compared to ~ 64 GPa and ~ 4 GPa in the enamel region (Fig. 6B and D), respectively. However, the property maps of *Sarcosuchus* did not show a clear gradation of elastic modulus and hardness from dentin layer to enamel layer, as compared to *Suchomimus* (Fig. 7A and C). In *Sarcosuchus* tooth, elastic modulus and hardness in dentin region was ~ 85 GPa and ~ 3.8 GPa, as compared to ~ 95 GPa and ~ 4.5 GPa in the enamel region respectively (Fig. 7B and D). The depth of penetration in nanoindentation experiments was in the range of $\sim 400\text{--}700$ nm and the average values of mechanical properties were slightly lesser ($\sim 5\text{--}10\%$) compared to microindentation experiments.

3.5. Fracture toughness

High load indentation experiments resulted in the crack formation

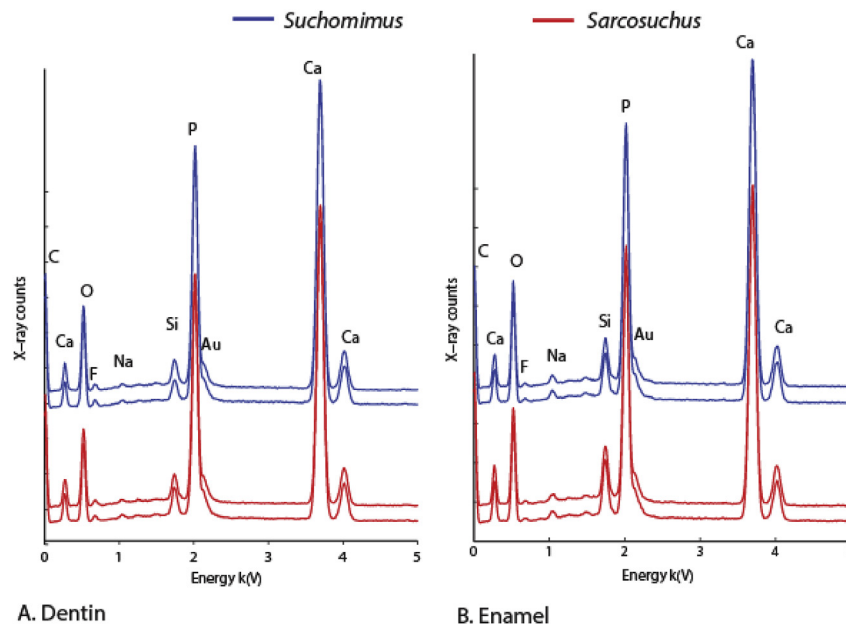


Fig. 2. Spectra from X-ray microanalysis showing the elements present in different regions of the species. A) Dentin region. B) Enamel region.

Table 1
Elemental composition of the teeth obtained from X-ray microanalysis.

	<i>Suchomimus tenerensis</i>		<i>Sarcosuchus imperator</i>	
	Wt%	At%	Wt%	At%
Oxygen	26.1 ± 1.4	45.3 ± 1.7	26.8 ± 1.0	45.4 ± 1.2
Calcium	44.4 ± 0.9	30.8 ± 0.9	44.3 ± 0.7	29.9 ± 0.7
Phosphorus	16.9 ± 0.5	15.2 ± 0.5	16.9 ± 0.4	14.8 ± 0.4
Carbon	2.1 ± 0.4	5.0 ± 0.8	2.2 ± 0.2	5.1 ± 0.4
Fluorine	1.1 ± 0.5	2.5 ± 0.8	2.5 ± 0.8	3.5 ± 1.1
Sodium	0.5 ± 0.3	0.6 ± 0.3	0.3 ± 0.1	0.3 ± 0.2
Silicon	0.1 ± 0.1	0.1 ± 0.1	< 0.1 ± 0.1	< 0.1 ± 0.1

Table 2
Elemental composition (at%) variation in dentin and enamel of the teeth obtained from X-ray microanalysis.

	<i>Suchomimus tenerensis</i>		<i>Sarcosuchus imperator</i>	
	Dentin	Enamel	Dentin	Enamel
Fluorine	1.6 ± 0.8	1.4 ± 0.7	3.4 ± 0.9	2.6 ± 1.6
Ca/P ratio	2.0 ± 0.1	1.9 ± 0.5	1.9 ± 0.4	1.9 ± 0.4

in both dentin and enamel regions. In *Suchomimus*, the observed damage was relatively less in the dentin demonstrating higher toughness (Fig. 8A). On the contrary, indentations in enamel region showed significant damage in terms of material chipping and longer cracks (Fig. 8C). A similar observation was made in *Sarcosuchus* except for that the size of the propagated cracks in dentin region was less prominent (Fig. 8B and D). Cracks in principle can propagate in the both axial and sagittal planes but we limited our study to cracks propagating in the axial plane to investigate the role of DEJ. Fracture toughness measurements showed that toughness is higher in dentin region compared to enamel region in all the species. *Suchomimus* had tougher dentin ($0.9 \pm 0.1 \text{ MPa m}^{1/2}$) and enamel ($0.6 \pm 0.1 \text{ MPa m}^{1/2}$) (Table 3).

Scanning electron microscope images were captured from the indentation region to examine fracture surface more clearly from high load fracture experiments. Cracks generated in the dentin region were much smaller and there was no material removal from surrounding region of the indentation region (Fig. 9A and B). In addition, cracks propagated in dentin region of *Suchomimus* were smaller and feeble as compared to the dentin regions of *Sarcosuchus*. All the indentations in enamel region resulted in a fracture with the removal of material from the adjacent region to indentation location as seen in Fig. 9 (C-D).

An additional set of indentations were performed close to DEJ for examining crack propagation from enamel to dentin. This observation closely mimics the general loading conditions of teeth where stress is generated on the outer surface of enamel during contact with diet or

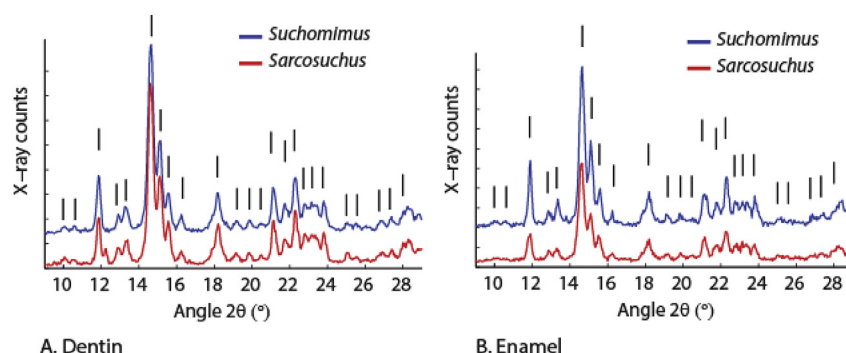


Fig. 3. Spectra from X-ray diffraction showing the peaks corresponding to the fluorapatite present in different regions of the species. A) Dentin region. B) Enamel region.

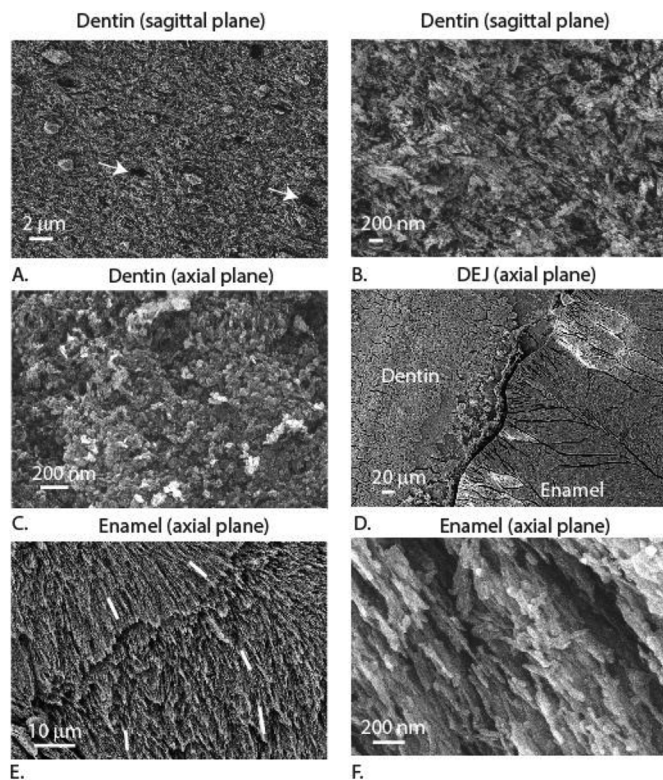


Fig. 4. Scanning electron micrographs of *Suchomimus* tooth internal microstructure. A) Dentin tubules (white arrows). B) Dentin microstructure in the axial plane. C) Dentin microstructure in the sagittal plane. D) Wavy pattern at the DEJ. E) Densely packed prismless enamel crystallites and change in orientation (white lines). F) Microstructure of the elongated enamel crystallites.

particulate matter attached to the diet. Thus, we performed indentation fracture experiments in enamel region in the proximity of DEJ to observe crack propagation behaviour through DEJ. In all the tooth samples, cracks appeared to propagate towards DEJ but partially deflected as they approached the junction without entering deep into the dentin region (Fig. 10A and B). In the enamel region the damage appeared to be more in terms of material removal due to brittle fracture.

3.6. Scratch testing

Scratch test results are presented using scratched surface image and indenter penetration depth. In *Suchomimus*, the scratched surfaces clearly show less wear on outer enamel layer as compared to the inner dentin layer (Fig. 11A). This was supported by the scratch depth results with less penetration in outer layers. On the contrary, the scratched surface of *Sarcosuchus* tooth did not show a significant difference between dentin and enamel layer, as seen from the scratch depth profile (Fig. 11B). The overall difference in wear depths between dentin and enamel regions is relatively higher in *Suchomimus* (Fig. 11C and D). We presented the values of coefficient of friction, hardness and fracture toughness (Table 4), to investigate their role on the scratch resistance. The coefficients of friction were observed to be almost similar in both the cases, which are attributed to same sample preparation technique resulting in similar surface roughness values. The hardness values were higher in enamel region as compared to dentin region in *Suchomimus*, also supported by the observed higher penetration depths in the scratch tests.

4. Discussion

X-ray diffraction and microanalysis results show that the teeth are

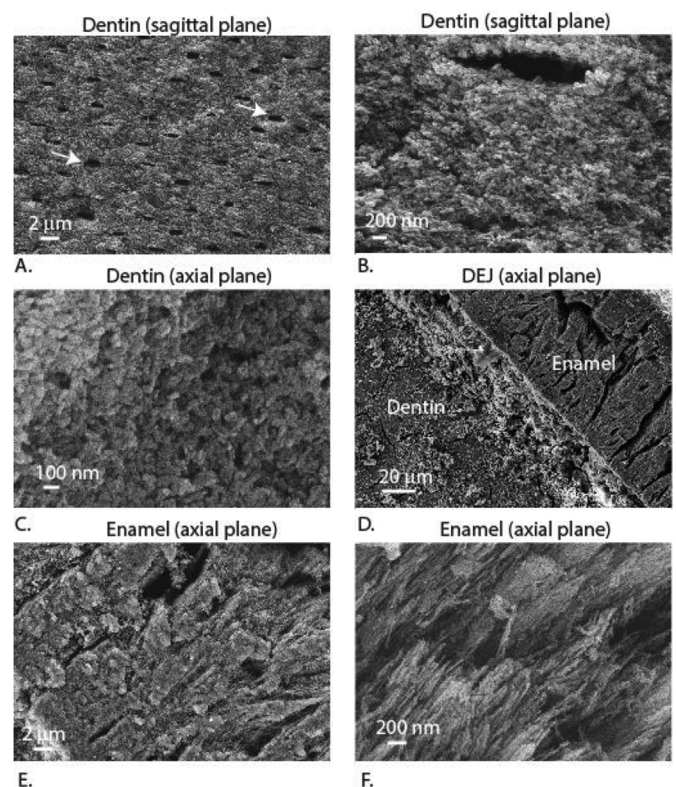


Fig. 5. Scanning electron micrographs of *Sarcosuchus* tooth internal microstructure. A) Dentin tubules. B) Dentin microstructure in the axial plane. C) Dentin microstructure in the sagittal plane. D) Linear interface at DEJ. E) Densely packed prismless enamel crystallites. F) Microstructure of the elongated prismless enamel crystallites.

mainly composed of fluorapatite, confirming previous studies in showing that hydroxyapatite is converted to fluorapatite during the diagenesis (Kohn et al., 1999). The fluorine peak in the X-ray microanalysis is coming from the fluorapatite. Furthermore, the X-ray diffraction peaks are similar to those found in an earlier study on fossilized dinosaur teeth (Lübke et al., 2015). The small differences in diffraction peaks can be attributed to the presence of varying amounts of incorporated ions such as sodium and carbonate in the apatite lattice (Enax et al., 2013). The measured hardness of *Suchomimus* tooth is in the same range of the herbivorous dinosaur *Triceratops* (Dentin: 3.1–5.3 GPa, Enamel: 5.6 GPa) (Erickson et al., 2015), and the retrieved tooth hardness of *Sarcosuchus* tooth is higher (~5 times in dentin region and ~2 times in enamel region) than that of the extant salt water crocodile *Crocodylus porosus* (Dentin: ~0.6 GPa, Enamel: ~3.15 GPa) Enax et al., 2013, determined using Vickers hardness test. The higher mechanical properties of fossil teeth, as compared to living teeth, can be attributed to increased mineralization.

A clear gradation was observed in the modulus and hardness of *Suchomimus* tooth, unlike in *Sarcosuchus*. The increased presence of fluorine in the dentin region as compared to the enamel of *Sarcosuchus* can be a contributing factor. Similar trend was observed in the scratch test, with *Suchomimus* tooth showing difference in the enamel and dentin, unlike in *Sarcosuchus*. Despite these differences in the gradation of the mechanical properties, crack deflection at the DEJ was observed in both the species. This can be attributed to the change of microstructure at the interface when the crack is propagating from enamel to dentin region. Also, the material removal during enamel fracture appears to be more in the direction of the enamel crystallite orientation. This is because the crack propagation is easier along the joining interface of enamel crystallites.

We note that the toughness values of the two fossilized species were

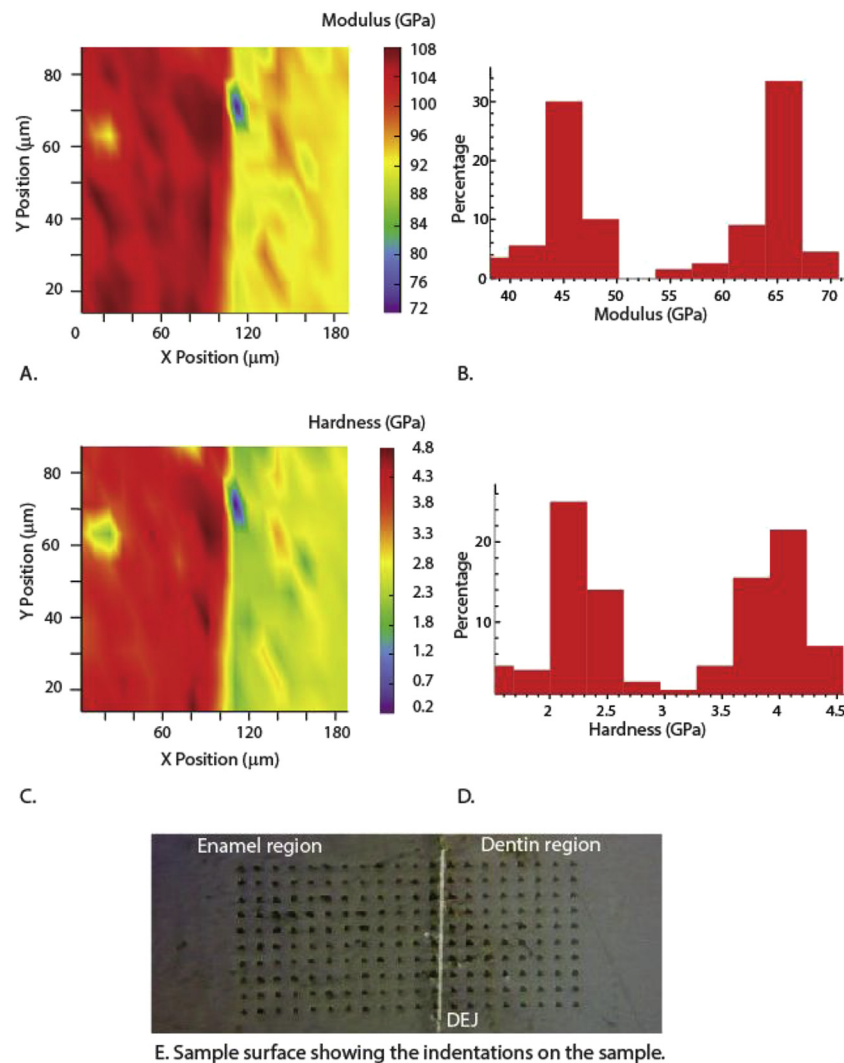


Fig. 6. *Suchomimus tenerensis*. A) Elastic modulus mapping across the layers. B) Corresponding elastic modulus values sorted into bins to show the variation and percentages. C) Hardness mapping across the layers. D) Corresponding hardness values sorted into bins to show the variation and percentages. E) Optical image showing the indented surface.

similar to the values of living human tooth dentin $\sim 1.79 \text{ MPa m}^{1/2}$ (Imbeni et al., 2003), elephant tusk, $1.6\text{--}2.6 \text{ MPa m}^{1/2}$ (Nalla et al., 2003), and mammal enamels, $0.7\text{--}1.06 \text{ MPa m}^{1/2}$ (Ayatollahi and Karimzadeh, 2013). We therefore infer that the toughness of the studied teeth when they were alive must have been higher, because the process of diagenetic mineralization increases the hardness and probably resulting in reduced toughness. Also, from a microstructural perspective, the enamel crystallite pattern differences in both the teeth could contribute to the observed differences in mechanical properties. In both the species, discontinuities in the prismless enamel pattern were observed, as reported in other studies (Sander, 1997; Sander, 2000). In *Suchomimus*, the enamel pattern appeared to diverge and in *Sarchosuchus* it appeared to be parallel type of crystallite, as described in an earlier study (Sander, 1999). Experiments performed on bovine teeth showed that crack arresting occurs in DEJ only when the crack initiation takes place in enamel region (Bechtel et al., 2010). Other studies (Wang et al., 2015) discussed the importance of the region between DEJ and dentin, the inter-globular porous space (IGS), in crack deflection and energy absorption during crack propagation (Bechtel et al., 2010).

Suchomimus teeth had lower elastic modulus when compared with *Sarcosuchus*, showing that they are less stiff. They are also more prone to wear as observed in the scratch test and the lower value of hardness to modulus ratio, but displayed better toughness characteristics. On the

contrary *Sarcosuchus* teeth are more stiff as they deform less; they are also harder to scratch, but could fracture more easily. Although the rarity of the investigated specimens prevents conducting the destructive tests performed in this study on a larger number of samples, the results obtained can be used to make some inferences on the teeth of the two species in the living condition. *Suchomimus tenerensis* was the most common large theropod in the Gadoufaoua fauna, with a snout of about 60 cm and body length of ca. 11 m (Sereno et al., 1998). In this species the teeth show fine wrinkling of the enamel (Sereno et al., 1998; Buffetaut, 2013) and are deep-rooted teeth, ideal for resisting large dorso-ventrally orientated biting forces and dissipation of energy through the skull (Hans-Dieter Sues et al., 2002). *Sarchosuchus imperator*, a pholidosaurid crocodylomorph, was another long-snouted giant predator in the Gadoufaoua fauna (Sereno et al., 2001; Broin and Taquet, 1966). With a snout of about 70 cm, and a total body length of ca. 12 m, *Sarchosuchus* had smooth and sturdy-crowned conical-round teeth, ideal for resisting large anteroposterior stress, more than on the mediolateral, and a generalized diet which would have included large terrestrial prey such as dinosaurs (Sues et al., 1999; Monfroy, 2017; Sloan, 2002). Its snout was compressed dorso-ventrally, rather than medio-laterally as in spinosaurids, but the overall mechanical properties of the snout in *Sarchosuchus* are more similar to those of theropods than those of other crocodylians, possibly because of similar diets

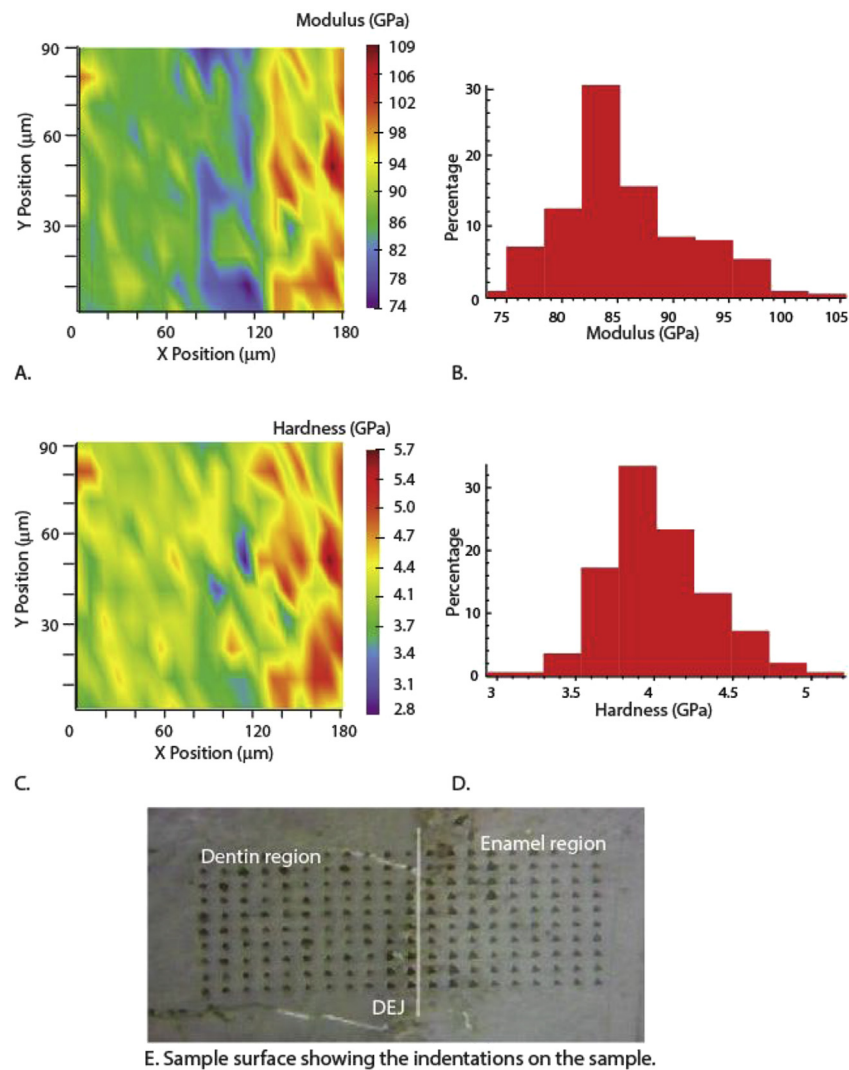


Fig. 7. *Sarcosuchus imperator*. A) Elastic modulus mapping across the layers. B) corresponding modulus values sorted into bins to show the variation and percentages. C) Hardness mapping across the layers. D) Corresponding hardness values sorted into bins to show the variation and percentages. E) Optical image showing the indented surface.

(Monfroy, 2017). Given these similarities, it is plausible to hypothesize that the respective ecological niches of *Suchomimus* and *Sarcosuchus* would have overlapped.

Our results might suggest that *Suchomimus* and *Sarcosuchus* used different strategies to cope with their dietary needs. *Suchomimus* teeth dispersed the energy of the bites by deforming and wearing much easily, but this allowed the teeth to fracture less frequently. On the contrary, during lifetime, *Sarcosuchus* teeth were extremely effective and relatively sharper given their higher modulus and hardness. However diagenetic differential alteration of the two teeth cannot be excluded without a better understanding of the processes involved. During diagenesis, alterations can occur at different length scales and recrystallization, partial dissolution, uptake of trace elements, erosion, and changes in porosity are in all expected to occur. With scarce knowledge on the amount of trace elements present in the modern reptile skeletal parts makes the interpretation difficult (Curie, 1997). In our study, using the observed elemental (Ca, F, Na) composition, we tried to comment on the taphonomic process. Earlier studies suggested that fluorine can also be used as a means of dating fossils and in contemporary tooth its content was found to be much less than one percent (DeManzanares et al., 2016). A comparison between the modern and fossilized hippopotamus showed increased levels of fluorine in the fossilized dentin as compared to the modern one (Brugmann et al.,

2012). High degree of diagenesis can also be attributed to the levels of sodium (Parker and Murphy, 1974), but we have not observed any significantly higher levels as compared to the extant crocodile. Calcium concentrations appear to have reached a saturated value as there were no significant differences between the dentin and enamel regions, and also between both the species (Table 1). Fluorine content (F) in the bone tissue that had undergone diagenesis, obtained from dating technique is estimated as (Lyman et al., 2012):

$$F = f(\text{SP}, K, H, T) \quad (2)$$

where, SP = skeletal part from the tissue part is derived, K = composition of burial environment, H = hydrology of the burial environment and T = temporal duration of the exposure. We compared our results with that of the extant crocodile teeth having fluorine content of 0.06 and 0.09 (Table 5), in dentin and in enamel respectively (Enax et al., 2013). We considered these values as a reference for fluorine levels in living archosaurs and thus estimated the amount of fluorine incorporated in enamel and dentin regions (Table 5). Because the samples were from the same skeletal part and deposits, same shared environment and are exposed to same time scales, we can attribute observed fluorine differences to the microstructure and permeability, in agreement with an earlier study (Lyman et al., 2012).

Elastic modulus values of fossilized mammalian long bones from an

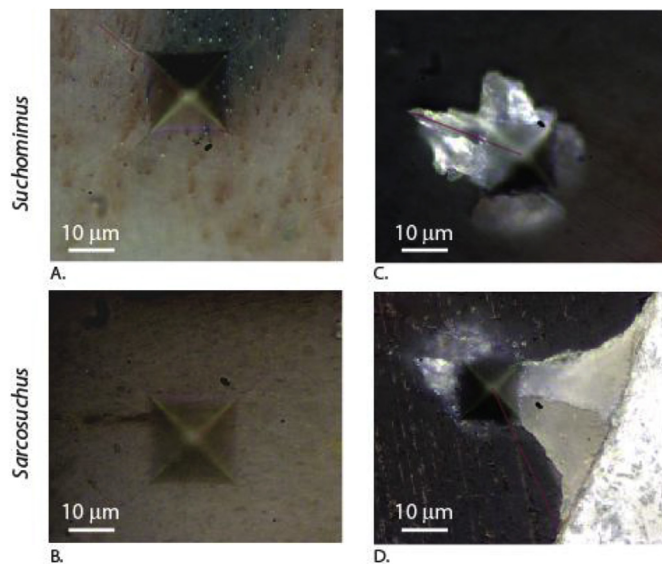


Fig. 8. Indentations showing fracture behaviour of teeth (red lines: crack lengths measurements). A-B) Feeble cracks extending from corners of indentations. C-D) Brittle fracture of enamel surface around the indentation and deflection of crack at the interface.

Table 3

Fracture toughness values of dentin and enamel regions from microindentation experiments.

Sample	Layer	Number of Indentations	Fracture toughness (MPa·m ^{1/2})
<i>Suchomimus tenerensis</i>	Enamel	4	0.5 ± 0.1
	Dentin	4	0.9 ± 0.1
<i>Sarcosuchus imperator</i>	Enamel	4	0.3 ± 0.1
	Dentin	4	0.6 ± 0.1

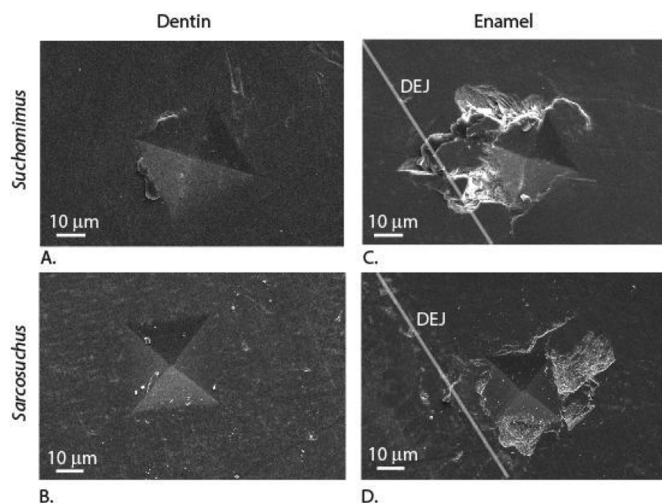


Fig. 9. Scanning electron micrographs of indentations. A-B) Feeble cracks extending from the end of indentation in dentin regions. C-D) Brittle fracture of enamel surface around the region of indentation showing removal of material in all the species.

age of 1 Ma to 50 Ma ranged from 35.0 to 89.1 GPa, respectively, and the increased modulus is attributed to the likely presence of calcium phosphate with trace elements (Olesiak et al., 2006). This is agreement with our observed higher mechanical properties. In principle, the Young's modulus of fluorapatite can reach a maximum of 104.96 GPa and a Vickers hardness of 5.58 GPa (Biskri et al., 2016). The estimated

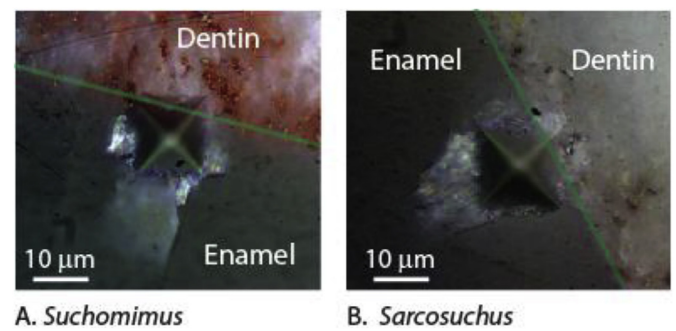


Fig. 10. Optical micrographs of indentations near the DEJ (green line) showing the fracture behaviour of the teeth. Chipping of material from enamel region due to brittle fracture is observed in the tested samples A) *Suchomimus tenerensis* B) *Sarcosuchus imperator*.

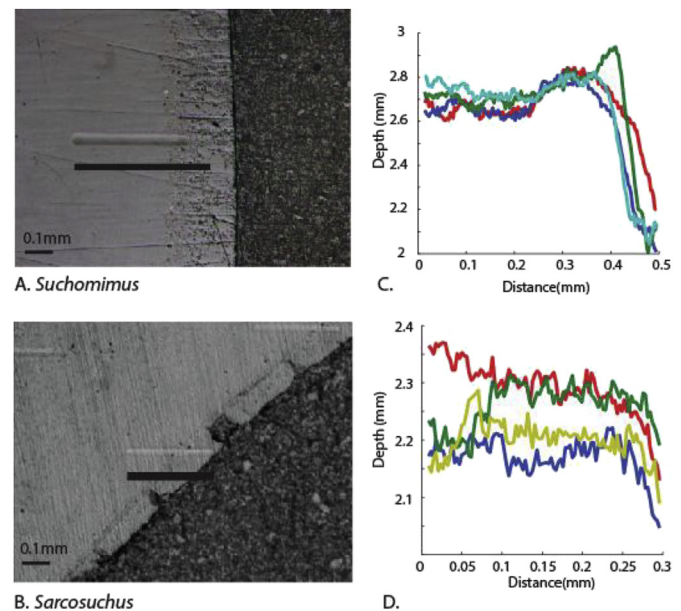


Fig. 11. A-B) Wear tracks (bright lines) produced on polished sections through different layers after scratching through a distance of 0.5 mm in *Suchomimus tenerensis* and 0.3 mm in crocodile *Sarcosuchus imperator*, as denoted by the black lines. C-D) Penetration depths from the scratch experiment on the corresponding teeth (applied normal force ~ 2 N).

hardness and elastic modulus of geological Durango fluorapatite were found to be 5.1 ± 1.3 GPa and 119 GPa, respectively (White et al., 2009).

5. Conclusions

Our study provides a first characterization of the fossilized teeth mechanical properties in a spinosaurid dinosaur, *Suchomimus tenerensis*, and an extinct pholidosaurid crocodylomorph, *Sarcosuchus imperator*. Mechanical gradients were highlighted between the enamel and dentin regions in *Suchomimus tenerensis* when elastic modulus, hardness, and wear of tooth were tested. In contrast, less significant difference in elastic modulus, hardness, and wear was measured in *Sarcosuchus imperatoris* tooth. Overall, *Suchomimus* teeth were found to be less stiff (lower elastic modulus), more prone to wear, but more tough, as compared to *Sarcosuchus*. These results can contribute to the understanding if there was any niche partitioning between two potential predatory competitors. However, much is still unknown concerning the changes underwent by organic material during diagenesis, making at present impossible to definitely conclude if the differences in the

Table 4
Scratch depth related properties (average values).

Sample	Dentin			Enamel		
	Friction coefficient	Hardness (GPa)	Fracture toughness (MPa·m ^{1/2})	Friction coefficient	Hardness (GPa)	Fracture toughness (MPa·m ^{1/2})
<i>Suchomimus tenerensis</i>	0.086	2.6	0.91	0.086	4.5	0.50
<i>Sarcosuchus imperator</i>	0.082	6.1	0.59	0.082	6.7	0.27

Table 5
Average values of elemental composition and mechanical properties for comparison between the fossilized specimens and the extant crocodile.

	<i>Suchomimus tenerensis</i> (fossilized)		<i>Sarcosuchus imperator</i> (fossilized)		<i>Crocodylus porosus</i> (extant) (Dauphin and Williams, 2008; Enax et al., 2013)	
	Dentin	Enamel	Dentin	Enamel	Dentin	Enamel
Fluorine (wt%)	1.3	0.93	2.52	2.43	0.06	0.09
Sodium (wt%)	0.68	0.27	0.30	0.21	0.78	1.01
Calcium (wt%)	44.48	44.33	44.38	44.24	16.5 -20	28-32.5
Ca/P ratio (wt%)	2.01	2.05	2.02	2.05	1.26	1.55
Hardness (GPa)	2.6	4.5	6.1	6.7	0.6	3.15

mechanical properties of *Suchomimus* and *Sarcosuchus* retrieved are the evidence of a real biological signal and therefore imply that the two species adopted different strategies when dealing with food processing, or are the result of disparate taphonomic histories.

Acknowledgments

The authors thank Simone Maganuco and Cristiano Dal Sasso (Museo di Storia Naturale di Milano) for making available the specimens. We are also grateful to Nicola Angeli (MUSE, Trento) for the help with SEM imaging and X-ray microanalysis. We would like to thank Gabriele Greco for help with SEM imaging of tooth microstructure. LK and NMP are supported by Fondazione Caritro under “Self-Cleaning Glasses” No. 2016.0278. NMP is supported by the European Commission under the Graphene Flagship Core 2 grant No. 785219 (WP14 “Composites”) and FET Proactive “Neurofibres” grant No. 732344 as well as by the Italian Ministry of Education, University and Research (MIUR) under the “Departments of Excellence” grant L.232/2016. MB acknowledges support from La Sportiva srl as part of the project “Dinomiti”.

References

Abràmoff, M.D., Magalhães, P.J., 2004. Image processing with ImageJ. *Biophot. Int.* 11, 36–42.

Ayatollahi, M.R., Karimzadeh, A., 2013. Nano-indentation measurement of fracture toughness of dental enamel. *Int. J. Fract.* 183, 113–118. <https://doi.org/10.1007/s10704-013-9864-x>.

Bechtel, S., Fett, T., Rizzi, G., Habelitz, S., Klocke, A., Schneider, G.A., 2010. Crack arrest within teeth at the dentinoenamel junction caused by elastic modulus mismatch. *Biomaterials* 31, 4238–4247. <https://doi.org/10.1016/j.biomaterials.2010.01.127>.

Biskri, Z.E., Rached, H., Boucheur, M., Rached, D., Aida, M.S., 2016. A comparative study of structural stability and mechanical and optical properties of fluorapatite (Ca5(PO4)3F) and lithium disilicate (Li2Si2O5) components forming dental glass—ceramics: first principles study. *J. Electron. Mater.* 45, 5082–5095. <https://doi.org/10.1007/s11664-016-4681-4>.

Broin, F. de, Taquet, P., 1966. Découvert d'un crocodilien nouveau dans le Crétacé inférieur du Sahara. *C. R. Acad. Sci. Paris* 262, 2326–2329.

Brüggmann, G., Krause, J., Brachert, T.C., Kullmer, O., Schrenk, F., Ssemmanda, I., Mertz, D.F., 2012. Chemical composition of modern and fossil Hippopotamid teeth and implications for paleoenvironmental reconstructions and enamel formation – Part 1: major and minor element variation. *Biogeosciences* 9, 119–139. <https://doi.org/10.5194/bg-9-119-2012>.

Buffetaut, Eric, 2013. An early spinosaurid dinosaur from the Late Jurassic of Tendaguru (Tanzania) and the evolution of the spinosaurid dentition. *ORYCTOS* 10, 1–8.

Buffetaut, E., Martill, D., Escuillie, F., 2004. Pterosaurs as part of a spinosaur diet. *Nature* 430 (6995), 33. <https://doi.org/10.1038/430033a>.

Charig, A.J., Milner, A.C., 1997. – *Baryonyx walkeri*, a fish-eating dinosaur from the Wealden of Surrey. *Bull. Hist. Mus. nat.* 53, 11–70.

Cuff, A.R., Rayfield, E.J., 2013. Feeding mechanics in spinosaurid theropods and extant crocodilians. *PLoS One* 8, 1–11.

Curie, J.P., 1997. In: *Encycl. Dinosaur*, [https://doi.org/10.1016/S0065-2628\(08\)60282-7](https://doi.org/10.1016/S0065-2628(08)60282-7).

Dauphin, Y., Williams, C.T., 2008. Chemical composition of enamel and dentine in modern reptile teeth. *Mineral. Mag.* 72, 247–250. <https://doi.org/10.1180/minmag.2008.072.1.247>.

De, Renzi M., Manzanares, E., Marin-monfort, M.D., Botella, H., 2016. Comments on “Dental lessons from past to present: ultrastructure and composition of teeth from plesiosaurs, dinosaurs, extinct and recent sharks. *RSC Adv.* 6, 74384–74388. <https://doi.org/10.1039/C6RA16316E>.

Enax, J., Fabritius, H.O., Rack, A., Prymak, O., Raabe, D., Epple, M., 2013. Characterization of crocodile teeth: correlation of composition, microstructure, and hardness. *J. Struct. Biol.* 184, 155–163. <https://doi.org/10.1016/j.jsb.2013.09.018>.

Erickson, G.M., Sidebottom, M.A., Kay, D.I., Turner, K.T., Ip, N., Norell, M.A., Sawyer, W.G., Krick, B.A., 2015. Wear biomechanics in the slicing dentition of the giant horned dinosaur *Triceratops*. *Sci. Adv.* 1, 1–7. <https://doi.org/10.1038/srep15202>.

Evans, A.G., Charles, E.A., Evans, A.G., Charles, E.A., 1976. Fracture toughness determinations by indentation. *J. Am. Ceram. Soc.* 59, 371–372. <https://doi.org/10.1111/j.1151-2916.1976.tb10991.x>.

Fortuny, J., Marcé-Nogué, J., Gil, L., Galobart, A., 2012. Skull mechanics and the evolutionary patterns of the otic notch closure in capitosaur (Amphibia: temnospondyli). *Anat. Rec.* 295, 1134–1146. <https://doi.org/10.1002/ar.22486>.

Hans-Dieter Sues, Frey, Eberhard, Martill, David M., Scott, Diane M., 2002. Irritator challenger, a spinosaurid (Dinosauria: Theropoda) from the lower cretaceous of Brazil. *J. Vertebr. Paleontol.* 22 (3), 535–547. [https://doi.org/10.1671/0272-4634\(2002\)022\[0535:ICASDT\]2.0.CO;2](https://doi.org/10.1671/0272-4634(2002)022[0535:ICASDT]2.0.CO;2).

He, L.H., Swain, M.V., 2009. Enamel-A functionally graded natural coating. *J. Dent.* 37, 596–603. <https://doi.org/10.1016/j.jdent.2009.03.019>.

Hendrickx, C., Hartman, S.A., Mateus, O., 2015. An overview of non avian discoveries and classification. *PalArch's J. Vertebr. Palaeontol.* 12, 1–73.

Hendrickx, C., Mateus, O., Buffetaut, E., 2016. Morphofunctional analysis of the quadrate of spinosauridae (dinosauria: theropoda) and the presence of Spinosaurus and a second spinosaurine taxon in the cenomanian of North Africa. *PLoS One* 11 (1), e0144695. <https://doi.org/10.1371/journal.pone.0144695>.

Holtz, T.R., 1998. Spinosaurus as crocodile mimics. *Science* 282, 1276–1277.

Hwang, S.H., 2005. Phylogenetic patterns of enamel microstructure in dinosaur teeth. *J. Morphol.* 266, 208–240. <https://doi.org/10.1002/jmor.10372>.

Hwang, S.H., 2010. The utility of tooth enamel microstructure in identifying isolated dinosaur teeth. *Lethaia* 43, 307–322. <https://doi.org/10.1111/j.1502-3931.2009.00194.x>.

Hwang, S.H., 2011. The evolution of dinosaur tooth enamel microstructure. *Biol. Rev.* 86, 183–216. <https://doi.org/10.1111/j.1469-185X.2010.00142.x>.

Imbeni, V., Nalla, R.K., Bosi, C., Kinney, J.H., Ritchie, R.O., 2003. In vitro fracture toughness of human dentin. *J. Biomed. Mater. Res. A* 66, 1–9. <https://doi.org/10.1038/nmat1323>.

Kellner, A., Mader, B., 1997. Archosaur teeth from the cretaceous of Morocco. *J. Paleontol.* 71, 525–527.

Kohn, M.J., Schoeninger, M.J., Barker, W.W., 1999. Altered states : effects of diagenesis on fossil tooth chemistry. *Geochem. Cosmochim. Acta* 63, 2737–2747.

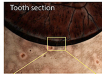
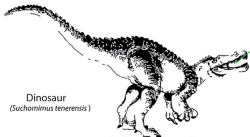
Lawn, B., Wilshaw, R., 1975. Indentation fracture - principles and applications. *J. Mater. Sci.* 10, 1049–1081. <https://doi.org/10.1007/BF00823224>.

Lübke, A., Enax, J., Loza, K., Prymak, O., Gaengler, P., Fabritius, H.-O., Raabe, D., Epple, M., 2015. Dental lessons from past to present: ultrastructure and composition of teeth from plesiosaurs, dinosaurs, extinct and recent sharks. *RSC Adv.* 5, 61612–61622. <https://doi.org/10.1039/C5RA11560D>.

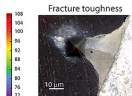
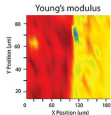
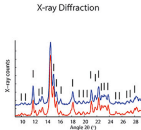
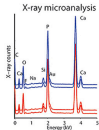
Lyman, R.L., Rosania, C.N., Boulanger, M.T., 2012. Comparison of fluoride and direct AMS radiocarbon dating of black bear bone from Lawson Cave, Missouri. *J. Field Archaeol.* 37, 226–237. <https://doi.org/10.1179/0093469012z.00000000021>.

Marshall, G.W., Balooch, M., Gallagher, R.R., Gansky, S.A., Marshall, S.J., 2001. Mechanical properties of the dentinoenamel junction: AFM studies of nanohardness, elastic modulus, and fracture. *J. Biomed. Mater. Res. A* 54, 87–95. <https://doi.org/10.1002/jbm.b.10011>.

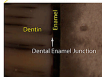
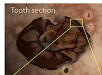
- 1002/1097-4636(200101)54:1<87::AID-JBM10>3.0.CO;2-Z.
- Martill, D.M., Cruickshank, A.R.I., Frey, E., Small, P.G., Clarke, M., 1996. A new crested maniraptoran dinosaur from the Santana Formation (Lower Cretaceous) of Brazil. *J. Geol. Soc. London*. 153, 5–8.
- Meyers, M.A., Chen, P.-Y., Lin, A.Y.-M., Seki, Y., 2008. Biological materials: structure and mechanical properties. *Prog. Mater. Sci.* 53, 1–206. <https://doi.org/10.1016/j.pmatsci.2007.05.002>.
- Monfroy, Quentin T., 2017. Correlation between the size, shape and position of the teeth on the jaws and the bite force in Theropoda. *Hist. Biol.* <https://doi.org/10.1080/08912963.2017.1286652>.
- Nalla, R.K., Kinney, J.H., Ritchie, R.O., 2003. Effect of orientation on the in vitro fracture toughness of dentin: the role of toughening mechanisms. *Biomaterials* 24, 3955–3968. [https://doi.org/10.1016/S0142-9612\(03\)00278-3](https://doi.org/10.1016/S0142-9612(03)00278-3).
- Olesiak, S.E., Oyen, M., Sponheimer, M., Eberle, J.J., Ferguson, V.L., 2006. Ultrastructural mechanical and material characterization of fossilized bone. 2006. MRS Fall Meet 975, 45–50.
- Parker, R.B., Murphy, J.W., 1974. Fluorine in fossilized bone and tooth: distribution among skeletal tissues. *Archeometry* 16, 98–102.
- Poole, D.F.G., 1957. The formation and properties of the organic matrix of reptilian tooth enamel. *Q. J. Microsc. Sci.* 3, 349–367.
- Rayfield, E.J., 2007. Finite element analysis and understanding the biomechanics and evolution of living and fossil organisms. *Annu. Rev. Earth Planet* 541–576. <https://doi.org/10.1146/annurev.earth.35.031306.140104>.
- Rayfield, E.J., 2011. Structural performance of tetanuran theropod skulls, with emphasis on the Megalosauridae, Spinosauridae and Carcharodontosauridae. *Special papers in Paleontology* 86, 241–253.
- Rayfield, E.J., Norman, D.B., Horner, C.C., Horner, J.R., Smith, P.M., Thomason, J.J., Upchurch, P., 2001. Cranial design and function in a large theropod dinosaur. *Nature* 409, 1033–1037. <https://doi.org/10.1038/35059070>.
- Rayfield, E.J., Milner, A.C., Xuan, V.B., Young, P.G., 2007. Functional morphology of spinosaur “crocodile-mimic” dinosaurs. *J. Vertebr. Paleontol.* 27, 892–901. <https://doi.org/10.1371/journal.pone.0065295>.
- Rubin, C., Krishnamurthy, N., Capilouto, E., Yi, H., 1985. Clinical Science: stress analysis of the human tooth using a three-dimensional finite element model. *J. Dent. Res.* 1408–1411.
- Sander, P.M., 1997. Non-mammalian synapsid enamel and the origin of mammalian enamel prisms: the bottom-up perspective. *Tooth enamel microstructure* 1.
- Sander, P.M., 1999. The Microstructure of Reptilian Tooth Enamel: Terminology, Function, and Phylogeny.
- Sander, P.M., 2000. Prismless Enamel in Amniotes: Terminology, Function, and Evolution. *Development, Function and Evolution of Teeth*. pp. 92–106. <https://doi.org/10.1017/CBO9780511542626.007>.
- Sereno, Paul C., Beck, Allison L., Dutheil, Didier B., Gado, Boubacar, Larsson, Hans C.E., Lyon, Gabrielle H., Marcot, Jonathan D., Rahut, Oliver W.M., Sadleir, Rudyard W., Sidor, Christian A., Varricchio, David D., Wilson, Gregory P., Wilson, Jeffrey A., 1998. A long-snouted predatory dinosaur from africa and the evolution of spinosaurids. *Science* 282, 1298. <https://doi.org/10.1126/science.282.5392.1298>.
- Sereno, Paul C., Larsson, Hans C.E., Sidor, Christian A., Gado, Boubé, 2001. The giant crocodyliform Sarcosuchus from the cretaceous of africa. *Science* 294 (5546), 1516–1519. <https://doi.org/10.1126/science.1066521>.
- Serrano-Fochs, S., De Esteban-Trivigno, S., Marcé-Nogué, J., Fortuny, J., Fariña, R.A., 2015. Finite element analysis of the cingulata jaw: an ecomorphological approach to armadillo's diets. *PLoS One* 10, e0120653. <https://doi.org/10.1371/journal.pone.0120653>.
- Shimizu, D., Macho, G.A., 2007. Functional significance of the microstructural detail of the primate dentino-enamel junction: a possible example of exaptation. *J. Hum. Evol.* 52, 103–111. <https://doi.org/10.1016/j.jhevol.2006.08.004>.
- Sloan, C., 2002. Supercroc and the Origin of Crocodiles. *National Geographic*, Washington (DC), pp. 55.
- Sues, H.-D., Frey, E., Martil, D.M., 1999. The skull of irritator challengerii (Dinosauria:Theropoda:Spinosauridae). *J. Vertebr. Paleontol.* 19 (3 Suppl. 1), 79A.
- Taquet, P., 1976. Géologie et paléontologie du gisement de Gadoufaoua (Aptian du Niger). *Cah. Palaontol.* 1976, 1–191.
- Taquet, P., Russell, D.A., 1998. New data on spinosaurid dinosaurs from the early cretaceous of the sahara. *Academie Des Sciences Paris Serie* 2.
- Teaford, M.F., Smith, M.M., Ferguson, M.W.J., 2006. *Development, Function and Evolution of Teeth*. Cambridge University Press.
- Therrien, F., 2005. Feeding behaviour and bite force of sibretoothed predators. *Zool. J. Linn. Soc.* 145, 393–426. <https://doi.org/10.1111/j.1096-3642.2005.00194.x>.
- Wang, C.C., Song, Y.F., Song, S.R., Ji, Q., Chiang, C.C., Meng, Q.J., Li, H.B., Hsiao, K., Lu, Y.C., Shew, B.Y., et al., 2015. Evolution and function of dinosaur teeth at ultra-microstructural level revealed using synchrotron transmission X-ray microscopy. *Sci. Rep.* 5, 11. <https://doi.org/10.1038/srep15202>.
- White, S.N., Luo, W., Sarikaya, M., Snead, M.L., Paine, M.L., Fong, H., 2009. Biological organization of hydroxyapatite crystallites into a fibrous continuum toughens and controls anisotropy in human enamel. *J. Dent. Res.* 80, 321–326. <https://doi.org/10.1177/00220345010800010501>.



Composition



Mechanical properties



Extinct Crocodile
(*Sarcosuchus imperator*)

<http://pyrogeoweb.free.fr/crocodile.htm>